Comprehensive Investigation of Structural and Optical Properties of Spin-Coated Reduced Graphene Oxide Thin Films

[1]Jayesh Suresh Jadhav, [2]Narendra Uttamrao Patil,
[3]Dnyaneshwar Daulatrao Lokhande

[1,2]Department of Physics and Research Centre, Maratha Vidya Prasarak Samaj's K.R.T. Arts, B.H. Commerce and A.M. Science (KTHM) College, Nashik, Maharashtra, India
[3]Maratha Vidya Prasarak Samaj's Arts, Science and Commerce College, Ozar (Mig), Niphad, Nashik

Abstract:
Reduced graphene oxide (rGO) thin films were successfully fabricated using a sol–gel-assisted spin-coating technique and thermal reduction. In this work, a comprehensive investigation of the structural and optical properties of spin-coated rGO thin films was carried out to understand the influence of the reduction process on film characteristics. Field Emission Scanning Electron Microscopy (FESEM) revealed a uniform, wrinkled, and layered sheet-like morphology with interconnected rGO flakes, indicating the formation of a continuous thin film. Energy Dispersive X-ray (EDX) analysis confirmed carbon as the dominant constituent with a significantly reduced oxygen content, verifying the effective reduction of graphene oxide. X-ray Diffraction (XRD) analysis showed a broad (002) diffraction peak corresponding to graphitic carbon, confirming partial restoration of the sp^2-hybridized structure with crystallite size of 53.65 nm. Optical studies using UV–Visible spectroscopy exhibited strong absorption in the ultraviolet region with a red-shifted π–π^* transition, indicating enhanced electronic conjugation in rGO. Fourier Transform Infrared (FTIR) spectroscopy demonstrated the substantial removal of oxygen-containing functional groups after thermal reduction, while Raman spectroscopy revealed prominent D and G bands, confirming defect-induced disorder and the presence of few-layer rGO sheets. The combined structural and optical analyses confirm the successful synthesis of rGO thin films with desirable properties, making them suitable for potential applications in optoelectronic devices, sensors and energy-related technologies.

Keywords: Reduced graphene oxide; Spin coating; optical analyses; optoelectronic; technologies.

1. INTRODUCTION

Graphene-based materials have attracted significant attention in recent years due to their exceptional electrical, optical, mechanical, and thermal properties, making them promising candidates for a wide range of applications including optoelectronics, sensors, energy storage devices, and transparent conducting electrodes. Among these materials, graphene oxide (GO) and reduced graphene oxide (rGO) have emerged as practical alternatives to pristine graphene because of their scalable synthesis, solution processability, and tunable physicochemical properties [1, 2]. rGO retains many desirable characteristics of graphene, such as high electrical conductivity and optical transparency, while offering ease of fabrication through chemical or thermal reduction routes [2].

The structural and optical properties of rGO are strongly influenced by synthesis methods, reduction conditions, and film fabrication techniques. Thin film deposition plays a crucial role in determining surface morphology, uniformity, crystallinity, and defect density, which directly affect the performance of rGO-based devices [2 3]. Among various deposition techniques, spin coating is widely preferred due to its simplicity, low cost, reproducibility, and ability to produce uniform and controllable thin films over large areas. Spin-coated rGO thin films are therefore of considerable interest for applications requiring homogeneous coatings and precise control over thickness and surface characteristics [3, 4].

The reduction of GO to rGO involves the partial removal of oxygen-containing functional groups, leading to the restoration of the sp^2-hybridized carbon network. However, this process also introduces structural defects and disorder, which significantly affect the optical absorption behavior, band structure, and electronic transitions in rGO. Consequently, a comprehensive understanding of the relationship between structural features and optical properties is essential for optimizing rGO thin films for device applications [3-5]. Advanced characterization techniques such as Field Emission Scanning Electron Microscopy (FESEM), Energy Dispersive X-ray spectroscopy (EDX), X-ray Diffraction (XRD), UV–Visible spectroscopy, Fourier Transform Infrared (FTIR) spectroscopy, and Raman spectroscopy are commonly employed to elucidate these properties in detail.

In the present work focuses on the comprehensive investigation of the structural and optical properties of spin-coated reduced graphene oxide thin films. The reduced graphene oxide thin films were fabricated using a sol–gel-assisted spin-coating technique followed by thermal reduction to obtain rGO. The study systematically examines the surface morphology, elemental composition, crystalline structure, functional groups, optical absorption behavior and defect characteristics of the rGO thin films. The results provide valuable insights into the successful formation of rGO, the extent of reduction and the correlation between structural features and optical response, thereby highlighting the potential of spin-coated rGO thin films for future optoelectronic and sensing applications.

2. EXPERIMENTAL WORK

2.1 Synthesis and preparation of thin films of rGO

All chemicals used in this study were of analytical reagent (AR) grade. Graphene oxide (GO) powder (50 mg) was dispersed in 100 mL of deionized water to obtain a GO sol with a concentration of 0.5 mg/mL, followed by ultrasonication for 45 minutes to achieve a uniform dispersion. Subsequently, 5 mL of tetraethyl orthosilicate (TEOS) was added dropwise to the GO sol under continuous magnetic stirring. To catalyze the sol–gel reaction, 1 mL of 0.1 M hydrochloric acid was then introduced into the mixture. The resulting solution was stirred for 2 hours at room temperature to form a stable and homogeneous sol. Prior to film deposition, glass substrates were sequentially cleaned with acetone and deionized water for 10 minutes each and then dried under an infrared (IR) lamp for 20–30 minutes. The prepared GO sol was deposited onto the cleaned glass substrates (2x 2cm) using a spin-coating technique at a rotation speed of 2000 rpm for 30 seconds. The coated films were pre-dried at 80 °C for 10 minutes under an IR lamp to remove residual solvents. This spin-coating and drying cycle was repeated two to three times to achieve the desired film thickness. Finally, the deposited GO thin films were thermally reduced to reduced graphene oxide by annealing at 300 °C for 1 hour in a muffle furnace [6-8].

2.2 Characterization techniques

The structural and optical properties of the reduced graphene oxide thin films were comprehensively investigated using a combination of FESEM, EDX, XRD, UV–Visible spectroscopy, FTIR and Raman spectroscopy. Field Emission Scanning Electron Microscopy (FESEM) was employed to examine the surface morphology, uniformity, and microstructural features of the rGO thin films. Energy Dispersive X-ray (EDX) analysis was used to determine the elemental composition of the films. X-ray Diffraction (XRD) analysis was carried out to study the crystalline structure, phase identification, and interlayer spacing of the films. Optical properties were investigated using UV–Visible spectroscopy, which provided information on optical absorption behavior of the rGO thin films. Fourier Transform Infrared (FTIR) spectroscopy was utilized to identify functional groups and chemical bonding, allowing assessment of the removal of oxygen-containing functional groups during thermal reduction. Raman spectroscopy was employed as a powerful tool to analyze the structural disorder and defect density in the rGO films through the evaluation of the D and G bands and their intensity ratio (ID/IG), thereby offering valuable insight into the degree of reduction and graphitic ordering. Together, these characterization techniques provided a detailed understanding of the structural integrity, chemical composition and optical response of the spin-coated rGO thin films.

3. RESULTS AND DISCUSSION

3.1 Field Emission Scanning Electron Microscopy analysis

Figure 1 shows the FESEM micrograph of the spin-coated reduced graphene oxide thin film. The image clearly reveals a crumpled, wrinkled, and layered sheet-like morphology, which is a characteristic feature of rGO obtained after thermal reduction of graphene oxide [8, 9]. The rGO sheets appear to be randomly stacked and interconnected, forming a porous network with numerous folds and edge planes. Such crumpling and restacking of graphene layers arise due to the removal of oxygen-containing functional groups during annealing, leading to the collapse of the GO sheets and partial restoration of the sp^2 carbon network [9, 10].

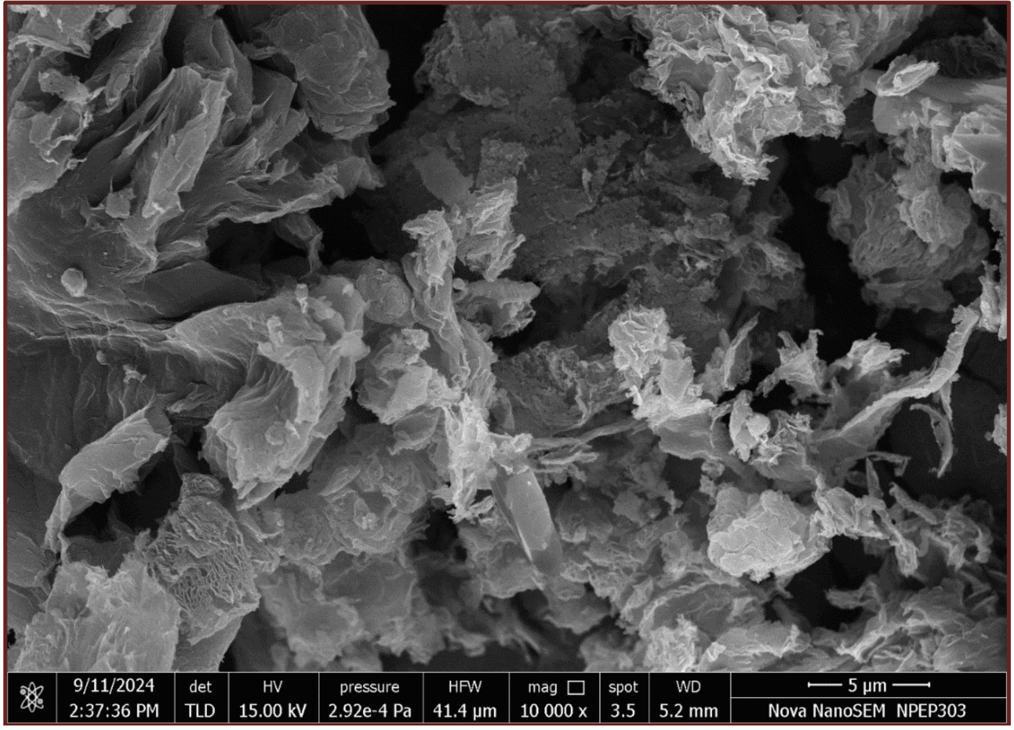

Fig. 1. FESEM image of rGO thin film

The specific surface area calculated my BET method (Eq. 1) and it was found to be 1.36 m^2/g.

Specific surface area = $6/\varrho d$ (Eq.1)

Where,

ϱ- Density of rGO and d –diameter of spherical particle.

The observed rough and highly textured surface indicates the presence of micro- and nano-scale voids between the overlapping rGO flakes, which contributes to the measured specific surface area. The uniform distribution of sheets across the surface suggests that the spin-coating process resulted in a homogeneous film coverage without large cracks or pinholes. The presence of sharp edges and thin lamellar structures confirms the exfoliated nature of rGO sheets rather than bulk agglomerates [10, 11]. This porous and wrinkled morphology is highly advantageous for applications such as optoelectronic devices, sensors, and energy storage, as it provides an increased number of active sites, enhanced surface interaction, and improved charge transport pathways. FESEM analysis confirms the successful formation of a continuous rGO thin film with favorable surface morphology and structural features [9-11].

3.2 Energy Dispersive X-ray analysis

Figure 2 illustrates the Energy Dispersive X-ray spectrum and corresponding elemental mapping of the reduced graphene oxide (rGO) thin film. The EDX spectrum is dominated by a strong carbon (C) peak, confirming that carbon is the principal constituent of the film. A comparatively weaker oxygen (O) peak is also observed, indicating the presence of residual oxygen-containing functional groups in the rGO structure [11, 12]. The reduced intensity of the oxygen peak relative to carbon suggests the effective thermal reduction of graphene oxide, resulting in partial removal of oxygen functionalities and restoration of the sp^2-hybridized carbon network [12, 13].

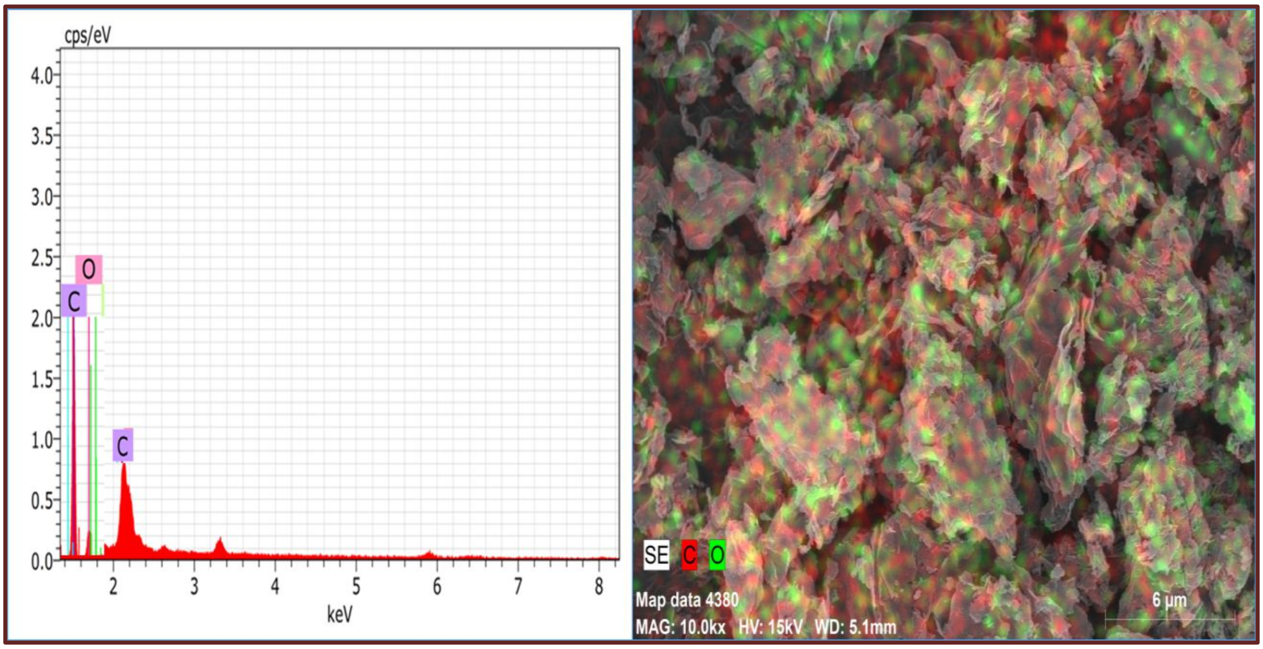

Fig. 2. EDX spectra of rGO thin film

The elemental mapping further reveals a uniform spatial distribution of carbon and oxygen across the film surface, indicating homogeneous film formation through the spin-coating process. Carbon is evenly distributed throughout the sample, while oxygen appears sparsely and uniformly dispersed, consistent with residual functional groups remaining after annealing. Such uniform elemental distribution is crucial for ensuring consistent structural and optical properties across the film. EDX analysis confirms the successful reduction of GO to rGO, high compositional purity and good film homogeneity [12-14].

3.3 X-ray Diffraction analysis

Figure 3 shows the X-ray diffraction pattern of the reduced graphene oxide thin film. The diffraction profile exhibits a prominent and broad peak centered at around $2\theta \approx 25.59°$, which corresponds to the (002) reflection plane of graphitic carbon and is in good agreement with the standard JCPDS card no. 41-1487 for graphite [15, 16]. The appearance of this (002) peak confirms the successful reduction of graphene oxide to rGO and the partial restoration of the graphitic layered structure after thermal annealing. Compared to pristine graphene oxide, which typically shows a sharp peak near 10–11° due to increased interlayer spacing caused by oxygen-containing functional groups, the shift of the peak to higher 2θ values indicates a decrease in interlayer spacing resulting from the removal of these functional groups during the reduction process [16, 17].

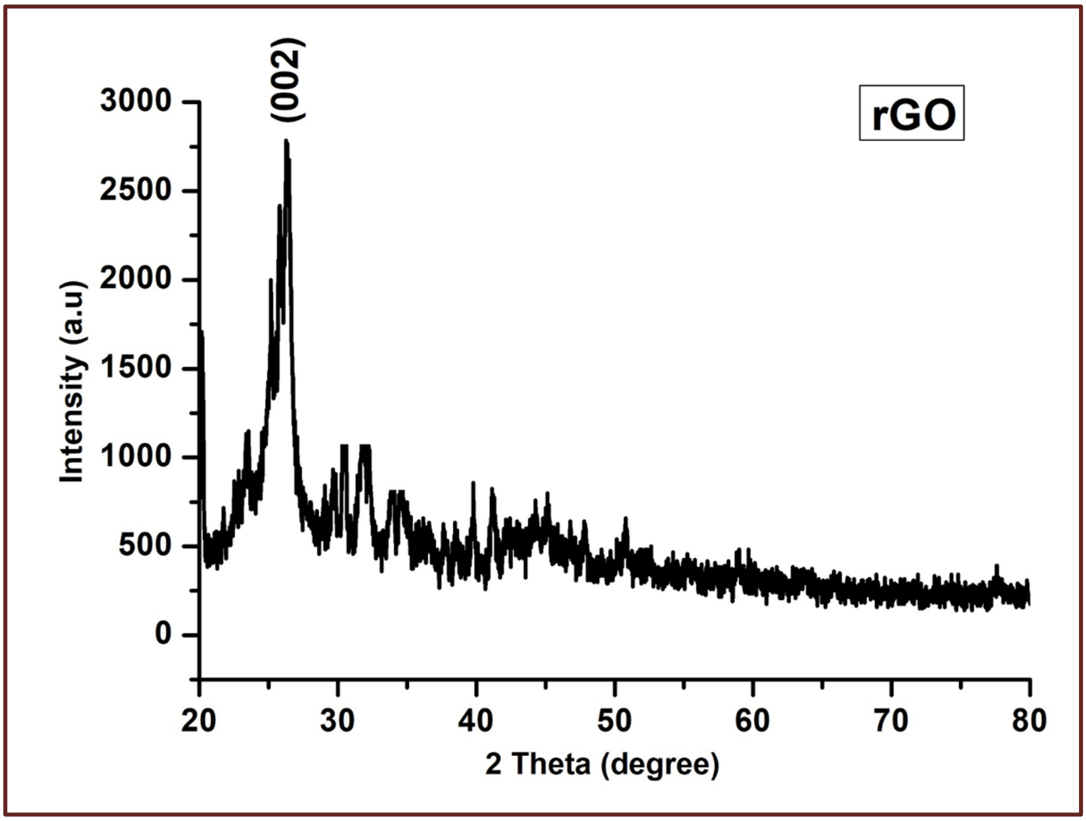

Fig. 3. XRD pattern of rGO thin film

The crystallite size of the rGO thin film was estimated to be 53.65 nm, calculated using the Debye–Scherrer equation (Eq.2) based on the full width at half maximum (FWHM) of the prominent (002) diffraction peak in the XRD pattern.

$$D = \frac{K\lambda}{\beta Cos\theta} \qquad \text{(Eq. 2)}$$

Where,
D- Crystallite size, K- Scherrer constant (0.9), β - Full width of half maxima (FWHM), and
λ - Wavelength of X source.

This nanoscale crystallite size indicates the formation of few-layer stacked graphene domains with limited crystallinity along the c-axis. The relatively moderate crystallite size suggests partial restoration of graphitic ordering after thermal reduction, while still retaining a degree of structural disorder due to residual defects and incomplete restacking of graphene layers. Such a crystallite size is typical for rGO materials and is advantageous for optical and electronic applications, as it balances good charge transport with a high density of edge sites and defects that enhance surface-related properties. The broad nature of the (002) diffraction peak suggests the presence of few-layered and turbostratically disordered graphene sheets, which is a characteristic feature of rGO [16-18]. This broadening also indicates reduced crystallite size along the c-axis and incomplete restacking of graphene layers, consistent with the wrinkled and exfoliated morphology observed in FESEM analysis.

3.4 UV–Visible spectroscopy analysis

Figure 4 shows the UV–Visible absorption spectrum of the reduced graphene oxide thin film recorded in the wavelength range of 200–800 nm. The spectrum exhibits a strong absorption in the ultraviolet region, with a broad absorption band centered around ~260–270 nm, which is attributed to the π–π* electronic transitions of aromatic C=C bonds in the sp^2-hybridized carbon network [18, 19]. The red shift of this absorption peak compared to graphene oxide (typically observed near ~230 nm) indicates the effective reduction of GO to rGO and the partial restoration of conjugated π-electron systems after thermal annealing [19, 20].

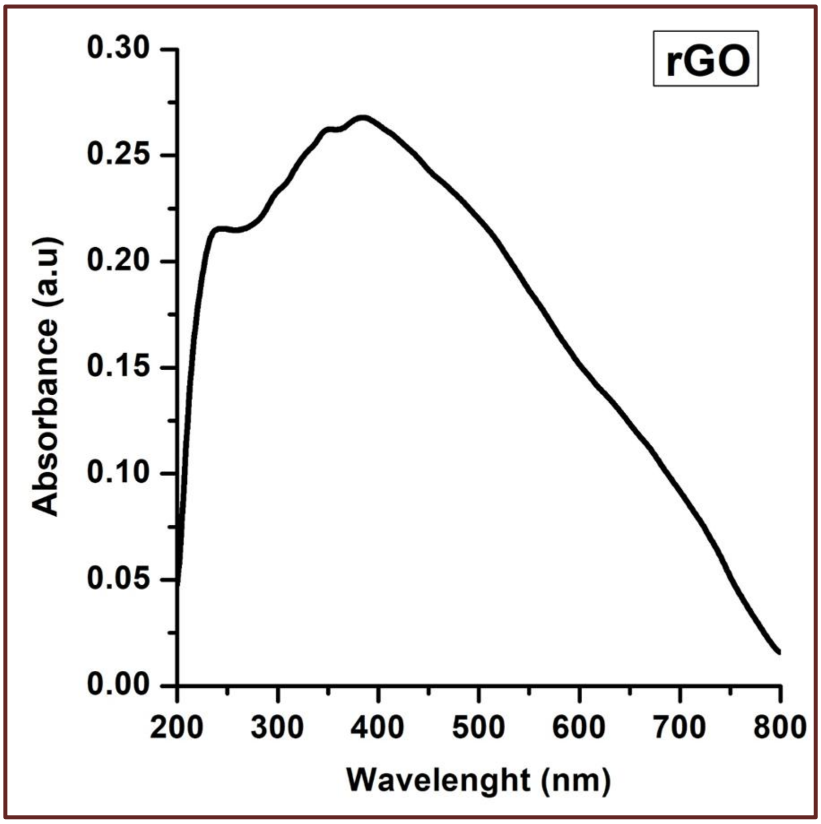

Fig. 4. Absorbance versus wavenumber plot of rGO thin film

In addition to the main UV absorption band, the spectrum shows a gradual decrease in absorbance toward the visible region, demonstrating that the rGO thin film possesses appreciable optical transparency in the visible range. This behavior is characteristic of rGO and is favorable for optoelectronic and transparent conducting applications [20, 21]. The absence of sharp absorption edges suggests the presence of localized states and structural disorder, which is consistent with the defect-rich nature of rGO.

3.5 Fourier Transform Infrared spectroscopy analysis

Figure 5 shows the Fourier Transform Infrared (FTIR) spectrum of the reduced graphene oxide (rGO) thin film recorded in the wavenumber range of 500–4000 cm^{-1}. The spectrum exhibits significantly weakened absorption bands compared to pristine graphene oxide, indicating the effective reduction of GO and removal of oxygen-containing functional groups during thermal annealing. The broad and low-intensity band observed around ~3400 cm^{-1} is attributed to the stretching vibration of residual hydroxyl (–OH) groups or adsorbed moisture on the rGO surface. A weak band near ~2920 cm^{-1} corresponds to C–H stretching vibrations, suggesting the presence of trace hydrocarbon species [20-23].

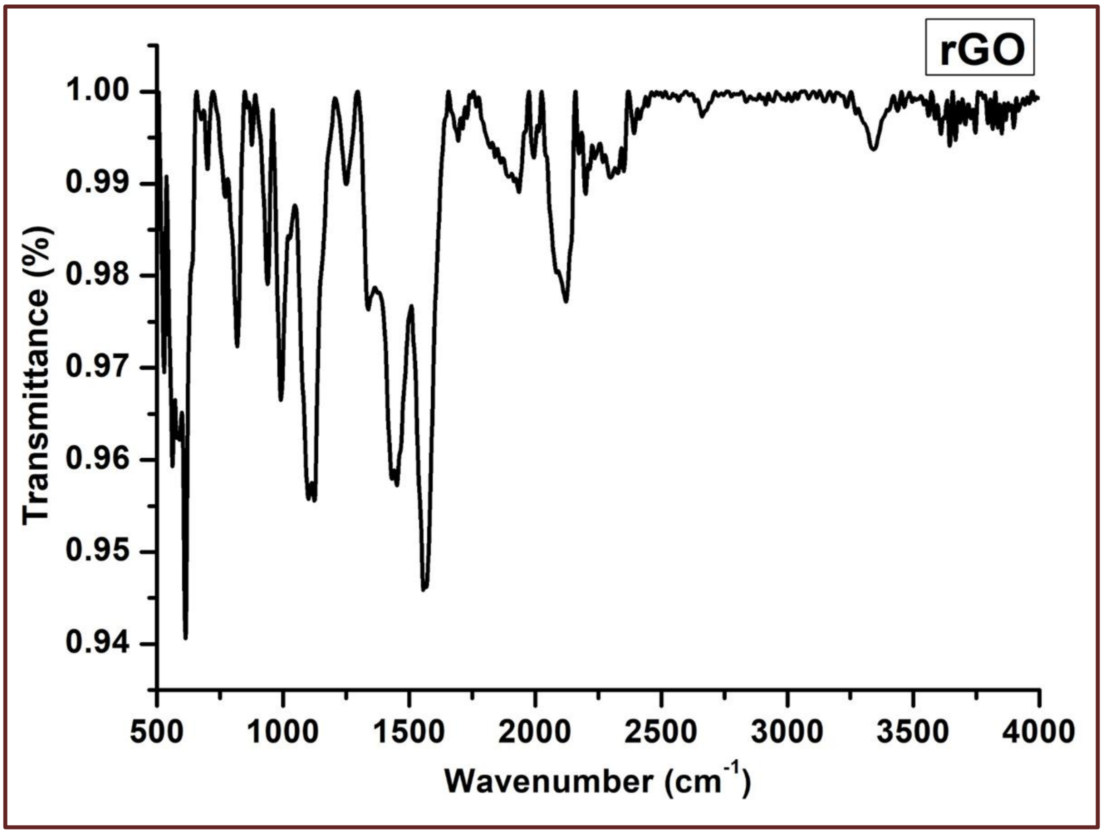

Fig. 5. FTIR spectra of rGO thin film

The absorption band observed around ~1620 cm^{-1} is assigned to the skeletal vibration of C=C bonds in the graphitic domains, confirming the restoration of the sp^2-hybridized carbon framework in rGO. The diminished intensity of peaks associated with oxygen functionalities, such as C=O stretching (~1720 cm^{-1}) and C–O or C–O–C stretching vibrations (1050–1250 cm^{-1}), further supports the successful reduction process. The overall high transmittance and weak vibrational features indicate a low concentration of functional groups and a more graphitic structure [23-25]. FTIR analysis confirms the effective conversion of GO to rGO and provides evidence for the partial elimination of oxygen-related groups, which is consistent with the XRD, EDX, and UV–Visible results.

3.6 Raman spectroscopy analysis

Figure 6 presents the Raman spectrum of the reduced graphene oxide thin film recorded in the Raman shift range of 500–3000 cm^{-1}. The spectrum exhibits two prominent characteristic peaks: the D band centered on ~1350 cm^{-1} and the G band located near ~1580 cm^{-1}. The D band arises from the breathing mode of sp^2 carbon atoms in rings and is associated with structural defects, edges, and disorder introduced during the oxidation and subsequent reduction processes [26-29]. In contrast, the G band corresponds to the in-plane stretching vibration of sp^2-bonded carbon atoms and is indicative of graphitic ordering within the rGO structure [30].

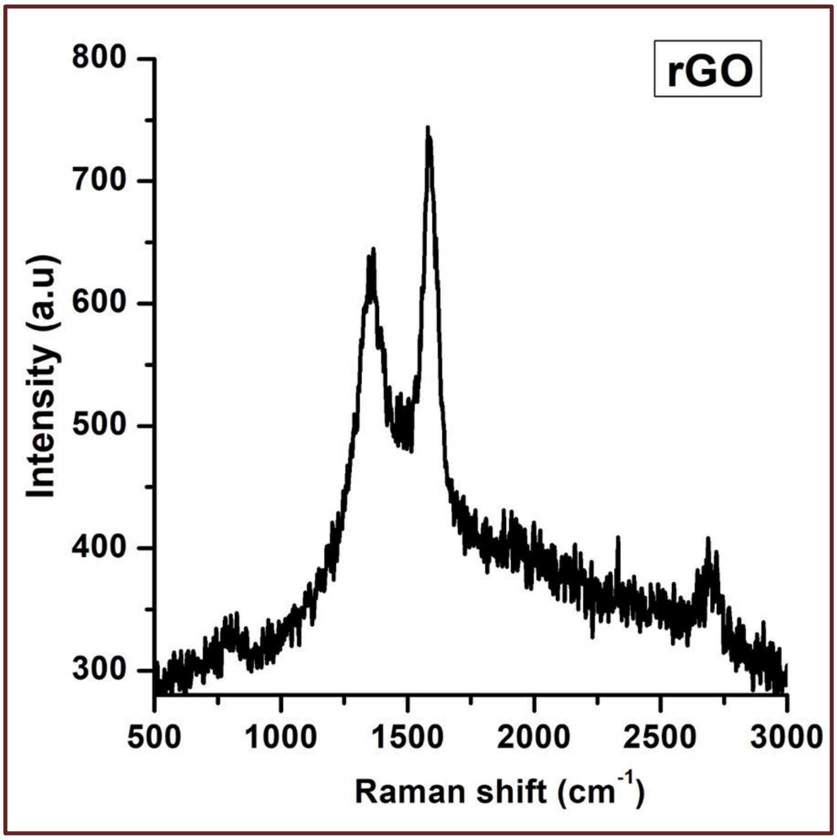

Fig. 6. Raman spectra of rGO thin film

The presence of a relatively intense D band alongside the G band indicates a defect-rich structure, which is typical for rGO due to residual oxygen functionalities and lattice imperfections remaining after reduction. The intensity ratio of the D and G bands (I_D/I_G) reflects the degree of disorder and the average size of sp^2 domains; an increased I_D/I_G ratio suggests the formation of smaller but more numerous graphitic domains following the reduction of GO. A weak and broadened 2D band observed around ~2700 cm^{-1} further confirms the formation of few-layer rGO sheets with turbostratic stacking rather than well-ordered graphite [29, 30]. The Raman analysis confirms the successful reduction of graphene oxide and partial restoration of the sp^2 carbon network while retaining structural defects [30, 31]. These defects and edge sites are beneficial for applications such as sensing and catalysis, as they enhance surface reactivity, while the restored graphitic domains support efficient charge transport.

CONCLUSIONS

i. Spin-coated reduced graphene oxide (rGO) thin films were successfully synthesized using a sol–gel-assisted method followed by thermal reduction.
ii. FESEM and EDX analyses confirmed uniform film formation with a wrinkled morphology and effective reduction of graphene oxide.
iii. XRD results revealed partial restoration of the graphitic structure with a crystallite size of 53.65 nm.
iv. UV–Visible, FTIR, and Raman studies confirmed enhanced electronic conjugation, removal of oxygen functional groups, and the presence of defect-rich few-layer rGO.
v. The obtained rGO thin films exhibit favorable structural and optical properties, making them suitable for optoelectronic and sensing applications.

Acknowledgment

The authors would like to express their sincere gratitude to the Principal, MVP’s K.R.T. Arts, B.H. Commerce and A.M. Science (KTHM) College, Nashik, Maharashtra, India, for providing the necessary infrastructure, laboratory facilities, and academic support required to successfully carry out this research work. The authors also gratefully acknowledge the constant encouragement and cooperation received from the management, Principal, and the Head of the Department of the institution. In addition, the authors extend their sincere thanks to the Central Instrumentation Facility (CIF), Savitribai Phule Pune University, Pune, for providing characterization facilities essential for this study.

REFERENCES:

1 Allen, M. J., Tung, V. C., & Kaner, R. B. (2010). Honeycomb carbon: A review of graphene. Chemical Reviews, 110(1), 132–145.
2 Bagri, A., Mattevi, C., Acik, M., Chabal, Y. J., Chhowalla, M., & Shenoy, V. B. (2010). Structural evolution during the reduction of chemically derived graphene oxide. Nature Chemistry, 2(7), 581–587.
3 Becerril, H. A., Mao, J., Liu, Z., Stoltenberg, R. M., Bao, Z., & Chen, Y. (2010). Evaluation of solution-processed reduced graphene oxide films as transparent conductors. ACS Nano, 4(8), 4636–4642.
4 Eda, G., & Chhowalla, M. (2010). Chemically derived graphene oxide: Towards large-area thin-film electronics and optoelectronics. Advanced Materials, 22(22), 2392–2415.
5 Stankovich, S., Dikin, D. A., Dommett, G. H. B., Kohlhaas, K. M., Zimney, E. J., Stach, E. A., … Ruoff, R. S. (2006). Graphene-based composite materials. Nature, 442(7100), 282–286.
6 Pei, S., & Cheng, H. M. (2012). The reduction of graphene oxide. Carbon, 50(9), 3210–3228.
7 Larciprete, R., Fabris, S., Sun, T., Lacovig, P., Baraldi, A., & Lizzit, S. (2011). Dual path mechanism in the thermal reduction of graphene oxide. Journal of the American Chemical Society, 133(43), 17315–17321.
8 Dreyer, D. R., Park, S., Bielawski, C. W., & Ruoff, R. S. (2010). The chemistry of graphene oxide. Chemical Society Reviews, 39(1), 228–240.
9 Eda, G., Fanchini, G., & Chhowalla, M. (2008). Large-area ultrathin films of reduced graphene oxide as a transparent and flexible electronic material. Nature Nanotechnology, 3(5), 270–274.
10 Gómez-Navarro, C., Weitz, R. T., Bittner, A. M., Scolari, M., Mews, A., Burghard, M., & Kern, K. (2007). Electronic transport properties of individual chemically reduced graphene oxide sheets. Nano Letters, 7(11), 3499–3503.
11 Rivera, H. A. T., Habermehl, A., Müller, C., Beck, S., Nieto, C. R., Sosa, G. H., & Quintana, M. E. (2017). Electrical and optical properties of reduced graphene oxide thin films deposited by spin coating. Applied Optics, 56(28), 7774–7780.
12 Kumar, P., & Kumar, A. (2018). Structural and optical properties of reduced graphene oxide thin films. Materials Research Express, 5(8), 085602.
13 Sreeja, V. G., Radhakrishnan, P., & Nampoori, V. P. N. (2016). Thickness dependent nonlinear optical properties of graphene oxide thin films. Optical Materials, 60, 321–327.
14 Politano, G. G., et al. (2022). Electrical and optical properties of graphene oxide and reduced graphene oxide thin films. Crystals, 12(2), 223.
15 Gomaa, M., et al. (2020). Optical properties of graphene oxide thin films reduced by laser irradiation. Applied Physics A, 126(3), 1–9.
16 Kaftelen-Odabaşi, H., et al. (2024). Structural and optical evaluation of reduced graphene oxide prepared by different reduction methods. Materials Science in Semiconductor Processing, 172, 108089.
17 Zabihi, F., et al. (2017). Sol–gel derived graphene–TiO_2 thin films: Structural and optical characterization. Catalysts, 7(3), 90.
18 Vallejo, W., et al. (2019). Graphene–TiO_2 thin films fabricated by sol–gel technique. Royal Society Open Science, 6(5), 190176.
19 Bui, T. T., et al. (2021). Fabrication and characterization of reduced graphene oxide thin films on glass substrates. Vacuum, 183, 109855.
20 Allagui, A., et al. (2016). Reduced graphene oxide thin films for electrochemical applications. Scientific Reports, 6, 21282.
21 Kim, J., et al. (2016). Wafer-scale patterning of reduced graphene oxide films. Scientific Reports, 6, 31276.
22 Smith, A. T., et al. (2019). Synthesis, properties, and applications of graphene oxide. Progress in Materials Science, 99, 1–44.

23 Razaq, A., et al. (2022). Graphene oxide and reduced graphene oxide based composites: A review. Materials, 15(3), 1012.

24 Purbayanto, M. A. K., et al. (2023). Ambient processed rGO thin films prepared by spin coating. Materials, 16(7), 2546.

25 Sedki, M., et al. (2022). Synthesis and characterization of graphene-like reduced graphene oxide thin films. Carbon Trends, 7, 100159.

26 AlShammari, A. S., et al. (2020). Optical and electrical properties of rGO-based thin films. Thin Solid Films, 709, 138225.

27 Kim, S. Y., et al. (2013). Thermal and optical behavior of reduced graphene oxide thin films. Journal of Applied Physics, 114(20), 203102.

28 Zhang, Y., et al. (2015). Optical absorption and electronic structure of reduced graphene oxide. Journal of Physical Chemistry C, 119(16), 9444–9451.

29 Ferrari, A. C., & Robertson, J. (2000). Interpretation of Raman spectra of disordered carbon. Physical Review B, 61(20), 14095–14107.

30 Malard, L. M., et al. (2009). Raman spectroscopy in graphene. Physics Reports, 473(5–6), 51–87.

31 Chen, D., et al. (2013). Graphene oxide: Preparation, functionalization, and electrochemical applications. Chemical Reviews, 113(8), 6027–6053.